Development of Test Procedures Based on Chaotic Advection for Assessing Polymer Performance in High-Solids Tailings Applications

Authors:

Allan Costine, Phillip Fawell, Andrew Chryss, Stuart Dahl, John Bellwood

Date Submitted: 2020-09-23

Keywords: consolidation, compressive yield stress, polyacrylamides, dewatering, flocculants, inline flocculation

Abstract:

Post-thickener polymer addition to initiate rapid tailings dewatering has gained considerable interest for tailings storage facility (TSF) management. However, the highly viscous and non-Newtonian rheology of dense suspensions presents unique challenges for mixing with polymer solutions. Such mixing is highly inefficient, often resulting in polymer overdosing and wide variations in deposited tailings characteristics, with the potential to significantly compromise TSF performance. In this study, a new type of mixer based on the principles of chaotic advection was used for treating kaolin suspensions with high molecular weight (MW) anionic copolymer solutions. Chaotic advection imparts efficient mixing by gently stretching and folding flows in a controlled manner, as opposed to random, high-shear flows associated with turbulent mixing, and this lower shear stress allows for the controlled formation of larger aggregate structures with vastly improved dewatering characteristics. A pre-conditioning pipe reactor prior to this mixer can also be advantageous in terms of providing a short burst of high shear for initial polymer distribution. Seven acrylamide/acrylate copolymers of a fixed anionic charge density (30%) spanning a distinct MW range, as characterized by intrinsic viscosity, were applied at elevated dosages to high-solids (20?30 wt %) kaolin suspensions in continuous flow through the chaotic mixer described above. Medium-to-high MW polymers were generally preferred, with further increases in MW resulting in significantly diminished dewatering outcomes. Direct analysis of polymer solution properties through oscillatory rheology gave a better indication of a polymer's potential performance compared with intrinsic viscosity, offering a more robust basis for polymer selection. This represented the first systematic study into the effects of polymer properties on deposition behavior after dosing at high solids, which was only possible through the ability to apply controlled shear across the entire suspension during sample preparation.

Record Type: Published Article

Submitted To: LAPSE (Living Archive for Process Systems Engineering)

Citation (overall record, always the latest version):	LAPSE:2020.1008
Citation (this specific file, latest version):	LAPSE:2020.1008-1
Citation (this specific file, this version):	LAPSE:2020.1008-1v1

DOI of Published Version: https://doi.org/10.3390/pr8060731

processes

MDPI

Article

Development of Test Procedures Based on Chaotic Advection for Assessing Polymer Performance in High-Solids Tailings Applications

Allan Costine [1,*], Phillip Fawell [1], Andrew Chryss [2], Stuart Dahl [1] and John Bellwood [3]

1 CSIRO Mineral Resources, Waterford, WA 6152, Australia; phillip.fawell@csiro.au (P.F.); stuart.dahl@csiro.au (S.D.)
2 CSIRO Mineral Resources, Clayton, VIC 3169, Australia; andrew.chryss@csiro.au
3 BASF plc, Hub 26, Charlesworth House, Hunsworth Lane, Cleckheaton BD19 4LN, UK; john.bellwood@partners.basf.com
* Correspondence: allan.costine@csiro.au; Tel.: +61-8-9334-8031

Received: 14 May 2020; Accepted: 20 June 2020; Published: 24 June 2020

Abstract: Post-thickener polymer addition to initiate rapid tailings dewatering has gained considerable interest for tailings storage facility (TSF) management. However, the highly viscous and non-Newtonian rheology of dense suspensions presents unique challenges for mixing with polymer solutions. Such mixing is highly inefficient, often resulting in polymer overdosing and wide variations in deposited tailings characteristics, with the potential to significantly compromise TSF performance. In this study, a new type of mixer based on the principles of chaotic advection was used for treating kaolin suspensions with high molecular weight (MW) anionic copolymer solutions. Chaotic advection imparts efficient mixing by gently stretching and folding flows in a controlled manner, as opposed to random, high-shear flows associated with turbulent mixing, and this lower shear stress allows for the controlled formation of larger aggregate structures with vastly improved dewatering characteristics. A pre-conditioning pipe reactor prior to this mixer can also be advantageous in terms of providing a short burst of high shear for initial polymer distribution. Seven acrylamide/acrylate copolymers of a fixed anionic charge density (30%) spanning a distinct MW range, as characterized by intrinsic viscosity, were applied at elevated dosages to high-solids (20–30 wt %) kaolin suspensions in continuous flow through the chaotic mixer described above. Medium-to-high MW polymers were generally preferred, with further increases in MW resulting in significantly diminished dewatering outcomes. Direct analysis of polymer solution properties through oscillatory rheology gave a better indication of a polymer's potential performance compared with intrinsic viscosity, offering a more robust basis for polymer selection. This represented the first systematic study into the effects of polymer properties on deposition behavior after dosing at high solids, which was only possible through the ability to apply controlled shear across the entire suspension during sample preparation.

Keywords: inline flocculation; flocculants; polyacrylamides; dewatering; compressive yield stress; consolidation

1. Introduction

The recovery of water from fine tailings in the mineral industry is a long-standing and well documented challenge for tailings storage facility (TSF) management [1–3]. Gravity thickening has been the main approach to concentrating tailings as it allows for the highest volumetric throughputs, but conventional thickeners typically produce underflows that have at best a low yield stress, and therefore need to be stored in tailings dams. More modern paste thickeners offer more powerful

rake mechanisms and the opportunity for greater sediment bed depths that then lead to high yield stress underflows [4].

While additional short-term water returns from paste thickening may be small, the reduction in tailings moisture content, combined with effective deposition practices, leads to a quicker drying time to form a load-bearing state. The best-known full-scale applications are from the thickening and neutralization of bauxite residues produced via the Bayer Process [5], for which solids concentrations at deposition are already quite high (often >50 wt %).

However, such advantages may not be fully achieved for fine clay-based tailings because of their propensity to retain water and consolidate slowly over time [6]. The plate-like structure of clays, and the fact that flocculants (under most conditions) only adsorb to their minor edge faces, lead to very low-density, fractal aggregate structures. The solids concentrations at which paste behavior is achieved may be <25 wt %, meaning that the paste is still mainly water (e.g., approximately 90% water by volume), and while such pastes can be deposited, liquefaction (where shocks such as earthquakes lead to the paste becoming fluid) can then be a concern. In the case of clay-based tailings from the Canadian oil sands industry, a combination of residual bitumen, high pH, and clay mineralogy results in suspensions that are difficult to thicken conventionally, but that also do not consolidate well over time [7]. As a consequence, there is a huge legacy issue in tailings that now require further dewatering prior to any rehabilitation.

The addition of high dosages of polymer (often significantly more than flocculant dosages applied in thickeners under feedwell conditions) to high solids tailings streams has been shown to generate greatly enhanced dewatering relative to what can be achieved from thickening alone, and this is the subject of several patents. McColl et al. [8] describe a process that takes existing thickened tailings and through the addition of a suitable reagent at high dosages, achieves rapid dewatering such that upon deposition, the water runs off freely; Gaillard and Poncet [9] describe related applications.

The mechanism by which enhanced dewatering is achieved by polymer dosing at high solids is poorly understood. McColl et al. [8] claim that the process forms "super-aggregates"—essentially a continuous network rather than individual aggregates. Optimal mixing is not addressed, but it is stressed that the advantages on deposition cannot be achieved by flocculating in a thickener, with the material produced then not conducive to pumping. Wells et al. [10] highlighted the need for the process to be done at high solids, and the importance of adding flocculant under high shear, with the subsequent tapering of shear to give the optimum discharge properties. Fawell [11] has contrasted the likely distinctions between this process and conventional flocculation at low solids concentrations, postulating that elevated polymer dosages in the former lead to high internal aggregate bridging that then favors chain relaxation and aggregate densification, but that was largely speculation on the basis of limited physical evidence.

As an addition to gravity thickening, the injection of polymer additives inline and immediately pre-discharge at the TSF has significant potential to accelerate water recycle, thereby offering environmental, capital, and footprint advantages. However, detailed studies into the process and the appropriate choice of flocculants are made difficult by high dosages, making it necessary to use higher flocculant concentration, and hence the dosed flocculant solution rheology becomes an issue. Additional mixing problems arise due to the non-Newtonian rheology of high-density suspensions, with small-scale testing typically done in stirred beakers, giving very poor control over the shear intensity and duration, which must contribute to considerable over-dosing. There are many papers appearing that purport to give insights on applications of the process to oil sands tailings and flocculant effects [12–15], but issues with the test procedures applied make their conclusions unconvincing.

A promising alternative to the turbulent mixing of high solids streams with polymer solutions is chaotic mixing. This approach has been shown to impart a rapid, complete mixing of highly viscous and rheologically complex materials (such as concrete suspensions) through a series of stretching and folding motions whilst using minimal energy and imparting minimal shear stress [16–19].

Given that a major weakness of studies into polymer-assisted tailings deposition is the almost inevitable poor control over the properties of the initially aggregated solids, a focus of this work was on the development of test procedures for producing well-characterized, repeatable thickened suspensions with selected aggregate properties. With reproducible mixing and dispersion of viscous polymer solutions in tailings suspensions, this preparative approach has a greater prospect of identifying polymer properties for optimum dewatering performance. In the first stage, the addition of an anionic copolymer solution to dense model tailings suspensions was examined experimentally using a low-shear chaotic mixer and a common laboratory bench-top impeller mixer. The characterization of aggregate properties included the real-time monitoring of aggregate dimensions with a focused beam reflectance measurement (FBRM) probe, real-time aggregate imaging, and deriving density information from the size and free settling of individual aggregates after dilution. Then, applications of the chaotic mixer were extended to investigating the effect on model tailings suspension dewaterability by applying a series of anionic polyacrylamides (PAMs) with different molecular weights. This enabled polymer performance over a wide range of conditions to be compared with the viscoelastic properties of the polymer solutions determined by oscillatory rheology. Then, the potential for such mixing in both laboratory testing and full-scale applications is discussed.

2. Materials and Methods

2.1. Substrate and Polymer Preparation

The kaolin clay used was acquired from Prestige NY Australia and has the composition shown in Table 1. Suspensions were prepared at 20 wt % (228 kg m^{-3}) and 30 wt % (369 kg m^{-3}) solids in 0.005 M $CaCl_2$ solution at 250 rpm for 8 h and allowed to equilibrate overnight. Some slight variations were observed between batches, and all direct comparisons of polymer activity were therefore performed with the same batch.

Table 1. Composition (wt %) of the kaolin clay used.

SiO_2	Al_2O_3	Fe_2O_3	CaO	TiO_2	MgO	K_2O	Na_2O
46.1	36.5	0.9	0.9	0.8	0.5	0.2	0.1

All the polymers studied are based on a conventional polyacrylamide/polyacrylate backbone (Figure 1). A commercial linear copolymer of approximately 30% anionic character and very high molecular weight (Magnafloc® 336) was used in the initial comparison of mixing approaches. For the comparison of polymer properties, BASF synthesized a set of non-commercial PAMs of a fixed anionic charge density (30%) that span a distinct range of MWs, as characterized by intrinsic viscosity [η]. The seven polymers had nominal [η] values of 9.1, 10.3, 12.2, 15.4, 17.2, 18.5, and 19.6 dL g^{-1}. [η] is related to the polymer weight-average molecular weight, Mw, by the Mark Houwink equation, $[\eta] = K \cdot M_w{}^{\alpha}$, where K and α are constants. The determination of [η] followed the procedures specified in ASTM D2857-95 'Standard practice for dilute solution viscosity of polymers'.

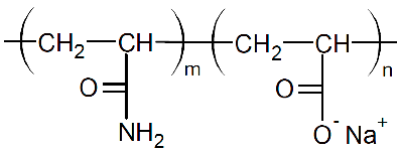

Figure 1. Structure of the acrylamide/acrylate copolymers studied.

Working polymer solutions (0.4–1.0 wt %, 6 L) were prepared fresh every three days (to minimize aging effects) by adding the appropriate mass of dry powdered polymer to the vortex produced in deionized water by an overhead stirrer (A310 impeller, diameter 160 mm, each blade 70 mm × 22 mm) in a 10 L container at approximately 250 rpm. Rapid stirring was continued for 30 min, with stirring

then reduced to a rate that just gave the continuous movement of the solution (80 rpm). This gentle agitation was maintained for 16 h. Working polymer concentrations were chosen to maintain a constant solution viscosity (and minimize dispersion effects), such that low MW polymers were applied at a higher concentration than the high MW polymers. Dosages are expressed as grams of polymer added per tonne of dry kaolin solids (g t^{-1}).

2.2. Polymer-Initiated Thickening and Dewatering

2.2.1. Initial Comparison of Chaotic vs. Impeller Mixing

To start an experiment, kaolin suspension at 0.5 L min^{-1} and polymer solution at the desired flowrate were pumped to separate inlets at the base of an acrylic mixing vessel (2 L capacity), as shown in Figure 2. The treated suspension exited the vessel via an angled overflow pipe (40 mm diameter). An adaptor positioned approximately 90° from the overflow pipe allowed the G400 FBRM probe (9.5 mm tip diameter) to be inserted into the mixing medium (not shown in Figure 2). Two types of mixer were tested: a chaotic (or topological) mixer and a pitched blade turbine mixer to produce flocculated solids with vastly different dewatering properties for further characterization and method development. The chaotic mixer imparted rapid complete mixing of the treated suspensions via a slow braiding motion of a series of vertical rods (280 × 6 mm). A central rod supports a lower set of arms that hold three fixed rods, which are rotating at 35 rpm. Three planetary rods trace out a cycloid pattern around the fixed rods at 52 rpm, giving complete mixing to the entire suspension under low shear conditions largely independent of rheology [20,21].

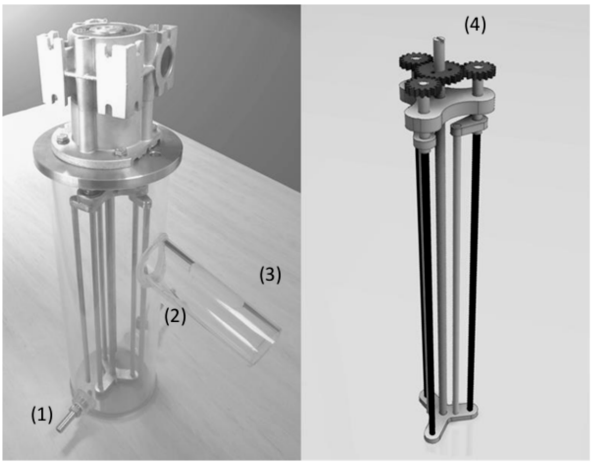

Figure 2. Experimental configuration showing the (1) suspension inlet, (2) polymer sparge positioned diametrically opposite the suspension inlet, (3) suspension outlet, and (4) planetary gearing system for the vertical rods used in the chaotic mixer.

The unbaffled impeller-based mixer (operated at 500 rpm) consisted of an overhead stirrer equipped with twin, three-pitched-blade impellers (each blade 30 mm long, 12 mm wide at the drive shaft, and tapered to 7 mm at the tip, angled at 45°, shaft 8 mm). Its main dimensions are as follows: the impeller diameter is 86 mm; the impeller-to-vessel diameter ratio (D/T) is 0.75; the liquid height-to-vessel diameter ratio (H/T) is 1.91; the clearance-to-impeller diameter ratio (C/D) is 0.23; and the distance between the twin impellers is 130 mm. While impeller-driven mixers are commonly used in laboratory studies for screening the effectiveness of a range of flocculant products, it is acknowledged that the current configuration (unbaffled, high D/T, and low C/D) and operational flocculation requirements (mixing intensity and duration) were not optimized to maximize water recovery.

In high-solids tailings applications, the residence times under shear are longer, and the sensitivity to the duration of applied shear is far more than in lower solids feedwell applications. In this context, an advantage of the low shear chaotic mixer as a laboratory tool is that it provides a uniform shear

history across the vessel, in contrast to the distinct zones of shear that will exist in a stirred tank, with the highest shear near the impeller. Continuous tests in the chaotic mixer have shown that flocculated solids are less sensitive to over-shearing due to the gentle braiding motion of the rotating rods, which offers scope to properly identify polymer properties that are best suited to the process. In the present study, the chaotic mixing method allowed polymer MW effects to be properly isolated from mixing effects.

When the FBRM chord length distribution and main statistics (total counts, unweighted, and length square-weighted means) indicated that a stable mixing state had been reached, a sample of conditioned suspension (0.5 L) was collected from the angled overflow pipe. Samples were collected in a rectangular deposition cell (500 × 100 × 100 mm), which was then placed on an elevated 4° slope table. Drainage holes in the base wall of the deposition cell allowed the mass of release water expelled from the treated suspension to be recorded every 1 min using an electronic balance and data logging software (Windmill Software Ltd., Manchester, UK). The drainage holes were covered with a fast-filtering cellulose paper (Macherey-Nagel^{TM} MN617 Nr4, 0.2 mm thick, 7–12 µm pore size) to prevent small particles/aggregates from entering the water receptacle. This was generally not an issue at dosages above 600 g t^{-1}, as the polymer-treated solids form a beach at the top of the deposition cell, which was then covered for the duration of the test to minimize evaporative losses.

Data-logging was concluded after 24 h, with most (>95%) of the recoverable water collected within the first two hours after deposition. The percentage of total water recovered was calculated from a mass balance of the release water and the water remaining within the sediment, as shown in Equation (1). Sediment moisture was calculated by the difference in mass of the wet and oven-dried (105°) solids. The repeatability in the dewatering measurements for selected experiments carried out under the same conditions was ± 3%.

$$\text{Water recovered } \% = \frac{\text{Water recovered}}{\text{Water in slurry} + \text{Water added in polymer solution}} \times 100 \quad (1)$$

2.2.2. Continuous Chaotic Mixing System with Tapered Shear

To start an experiment, kaolin suspension and polymer solution at the desired flowrates were pumped through a 2 m pre-conditioning coil (7.7 mm ID) before entering the chaotic mixer, as shown in Figure 3. When the FBRM statistics indicated that a stable mixing state had been reached (constant mean sizes), the treated suspension was collected for a 24 h gravity drainage test (4° slope), as described in Section 2.2.1. An advantage of this continuous system over other common batch mixers is that it can be readily applied to the study of tapered shear mixing regimes [10], particularly those involving two-stage polymer addition. There is little information available on the polymer property requirements for the initial short burst of rapid mixing and the subsequent slower, more quiescent mixing.

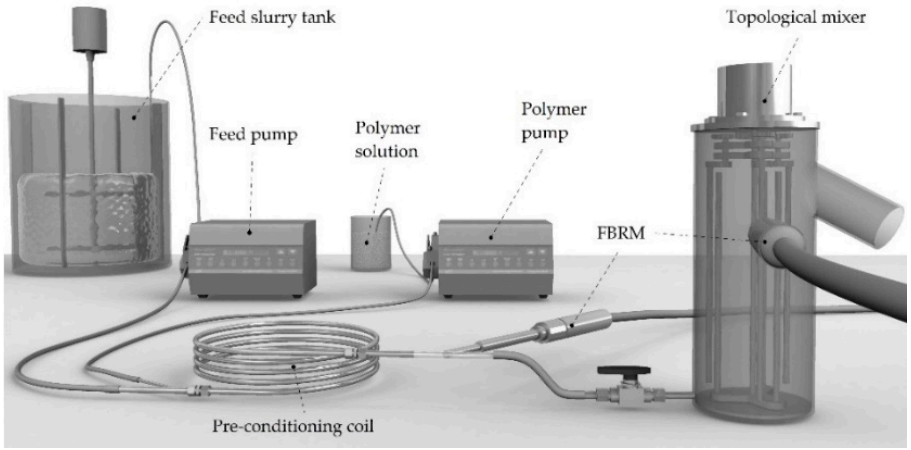

Figure 3. Optimized system to apply tapered shear for polymer addition to high solids suspensions.

2.3. Aggregate Characterization

Several different methods were used for the measurement of aggregate properties to thereby maximize information derived that is distinct from ultimate performance measures. Such an approach is desirable in any study of aggregates, but it is particularly important in this case where aggregate properties may change rapidly after deposition and the aggregation process is not well understood.

2.3.1. Focused Beam Reflectance Measurement

Conventional light scattering measurement of particle/aggregate size requires very high solids dilution, and while this may only be a minor inconvenience for dispersed particle systems, it makes sizing highly problematic for fragile aggregates. By relying on laser reflection rather than scattering, FBRM can provide real-time information without any requirement for solids dilution, and certainly not for most particle systems studied in mineral processing applications. Published applications at high solids are actually rare, although studies of alumina [22] and mixed silica–titania suspensions [23] at solids concentrations leading to elevated viscosities clearly demonstrate correlations with the extent of aggregation as monitored by FBRM.

A Mettler-Toledo FBRM model G400 with PI-14/206 probe was used (tip diameter 9.5 mm). FBRM utilizes a monochromatic laser beam scanning a circular path and focused at the external surface of a sapphire window. Reflections from particles or aggregates are measured as pulses when they exceed a threshold intensity, and thousands are measured every second, generating an unweighted chord length distribution. A chord length is the straight-line distance from one edge of a particle or aggregate to another edge. Length weightings may be applied to the chord length data to produce distributions that are more in keeping with the volume-based distributions obtained from laser light-scattering techniques [24]. When a steady state had been attained for the condition being studied, chord length distributions from 1 to 4000 µm were recorded every 2 s and averaged over five measurements. The advantages of using G-series FBRM instruments over previous-generation instruments in terms of greater sensitivity in concentrated particle systems and the detection of larger aggregate structures have been described elsewhere [25,26].

2.3.2. Floc Density Analysis

The size, shape, settling velocity, and density of individual aggregates were determined using a floc density analyzer (FDA) following the method of Farrow and Warren [27]. Sediment sample was diluted (as gently as possible to minimize aggregate rupture) with corresponding filtered release water to approximately 0.1 wt %. After thermostatting at 25 °C, dilute suspension was fed into the analysis cell of the FDA, and the taps closed to completely isolate the suspension to produce convection-free settling. Images of aggregate sedimentation under the influence of gravity within the cell were recorded. Aggregates with tails or filaments were not measured. Digital imaging and semi-automated image analysis allowed for strong statistical comparisons of hundreds of individual aggregates. An overall ellipsoidal geometry defined by the maximum vertical (a) and horizonatal (b) aggregate dimensions (with respect to the direction of settling) was assumed. The diameter of the sphere having a Stokes settling velocity equivalent to the ellipsoid was determined using the expression proposed by Happel and Brenner [28], valid for vertical-to-horizontal diameter ratios between 0.1 and 20,

$$d_{st} = \left[0.8248 + 0.168\left(\frac{a}{b}\right) + 1.033\times10^{-2}\left(\frac{a}{b}\right)^2 - 1.264\times10^{-3}\left(\frac{a}{b}\right)^3 + 3.728\times10^{-5}\left(\frac{a}{b}\right)^4\right]b. \quad (2)$$

If Stokes's Law is assumed, the density of an individual free settling aggregate (ρ_a) can be calculated as

$$\rho_a = \frac{18\mu}{g}\frac{U}{{d_{st}}^2} + \rho_l \quad (3)$$

where U is the terminal settling velocity of the aggregate of equivalent size (d_{st}); μ, ρ_l, and g are the fluid viscosity, fluid density, and the gravity constant, respectively.

2.3.3. Particle Vision and Measurement

Images of aggregates present within different sediments were acquired directly with a Particle Vision and Measurement (PVM) probe (Mettler-Toledo). This provides a highly focused strobing laser illumination of a stirred suspension (0.5 wt %), capturing an area of 660 × 880 μm (resolution 5 μm) with a limited depth of field, such that any aggregate in focus can be sized correctly. The PVM images were altered to enhance contrast and the colors were inverted to imitate the back-lighting conditions used in the FDA.

2.3.4. Rheological and Compressibility Characterization

Oscillatory rheology was carried out on polymer solutions using a Discovery Hybrid Rheometer HR-3 (TA Instruments, New Castle, DE, USA) equipped with two stainless steel parallel plates (diameter 60 mm). The sample temperature was controlled at 30 ± 0.1 °C by a Peltier system. For each polymer solution (0.1 wt %), the linear viscoelastic region (LVR) was determined via a stress sweep at a fixed frequency. Once determined, a frequency sweep from 0.1 to 100 rad s^{-1} was performed at a stress value selected from within the LVR. Rheological parameters were obtained directly from the manufacturer-supplied computer software (TRIOS, TA Instruments).

The compressibility of selected treated suspensions was measured using a stepped-pressure filtration rig [29]. Suspension was pressurized in a compression cell, forcing liquid out through a filter membrane at the cylinder base. The filtration pressure was monitored using a transducer mounted flush in the piston face. Movement of the piston was tracked by a linear encoder with a spatial resolution of 10 μm. The pressure control system allows pressures from 1 to 400 kPa to be applied. At the conclusion of each pressure step, the resulting cake at its characteristic solids concentration has a compressive yield stress equivalent to the applied pressure.

3. Results and Discussion

3.1. The Impact of Applied Mixing

3.1.1. Chord Length Distributions and Dewatering Performance

Figure 4 plots the unweighted chord length distributions and the corresponding net water removal measured for 20 wt % kaolin suspension as a function of polymer dosage and mixer type. The unweighted chord length distributions offer greater sensitivity to the number of particles within the suspension, in this case illustrating how increments in polymer dosage led to a progressive reduction in counts and an increase in apparent sizes. The magnitude of this effect was greatest for the chaotic mixer, although the impeller mixer displayed superior fines capture at lower dosages due to the rapid dispersion of the polymer throughout the suspension. However, the excessive shear that is hard to avoid with impeller mixing can lead to chain rupture and aggregate breakage, limiting the growth of larger aggregate structures, and it is this point that appears to be the key toward maximizing dewatering efficiency.

Polymer-initiated thickening by chaotic advection led to a doubling in net water recovery after 2 h compared with high-shear impeller mixing, as shown in Figure 4C,D. It is emphasized that the performance of the impeller mixer was not optimized for maximum water recovery—the results show the range of response that can be expected from laboratory-scale mixers involving uncontrolled turbulence and low-shear chaotic advection. For both mixers, increasing the polymer dosage over the range 400–1000 g t^{-1} resulted in additional water recovery, although further increases in dosage to 1200 g t^{-1} led to water entrapment, particularly for the chaotic mixer. In this case, streaks of unreacted polymer were clearly visible during mixing, which was evidenced by inefficient fines capture and a reduction in apparent sizes. In all cases, the dewatering efficiency appeared to be directly related to the real-time chord length distributions measured during deposition, with both the fines content and aggregate size contributing to the extent of water recovery.

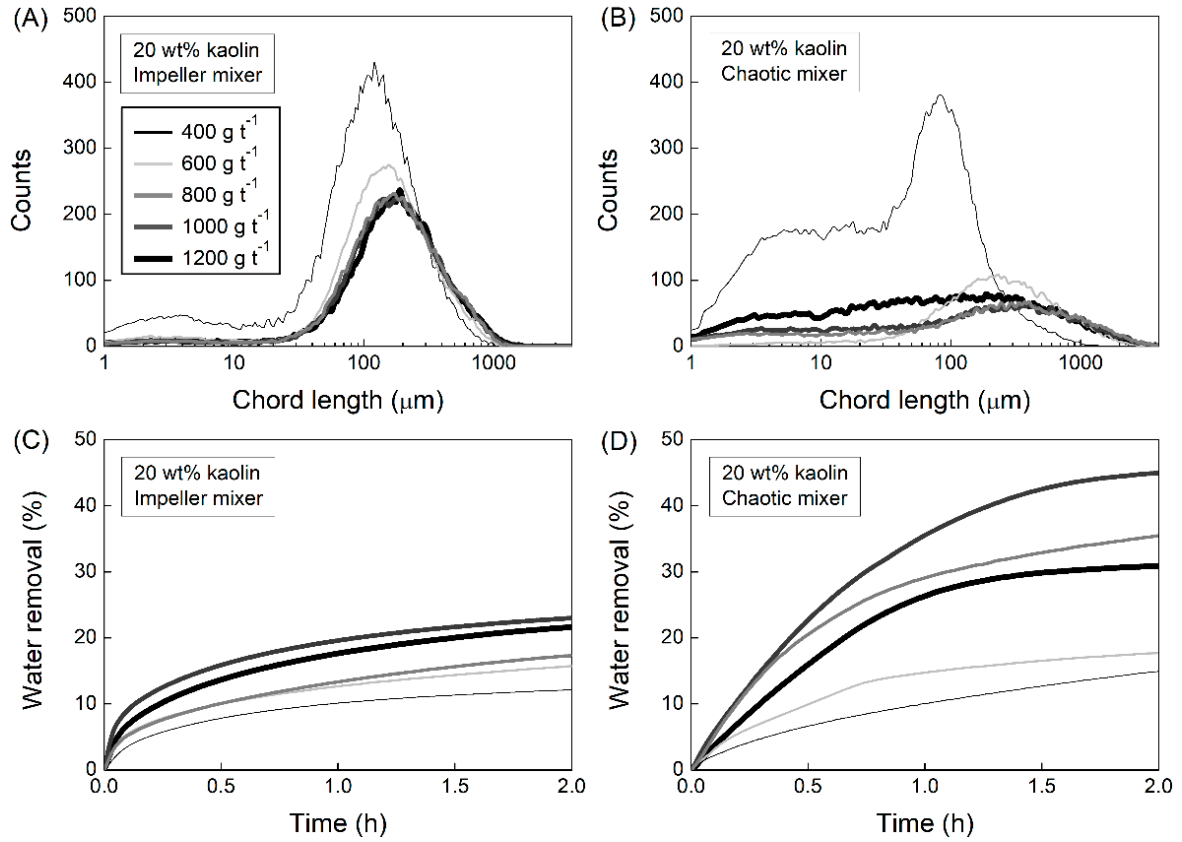

Figure 4. (**A**,**B**) Unweighted chord length distributions for 20 wt % kaolin as a function of Magnafloc® 336 dosage and mixer type. (**C**,**D**) Corresponding net water recovered after 2 h.

The mean-square weighted chord length distributions better capture the relative volumetric contributions of the aggregated solids, while being insensitive to the presence of any remaining unaggregated fine solids. Therefore, increases in aggregate size for reactions with the chaotic mixer are much more apparent in Figure 5, which shows a significant shift in the peak size to larger values (shaded area) as the dosage was increased. For example, at a polymer dosage of 1000 g t^{-1}, use of the impeller mixer led to unweighted and square-weighted means of 221 μm and 549 μm, respectively. The corresponding values for the chaotic mixer under the same conditions were 327 μm and 1650 μm.

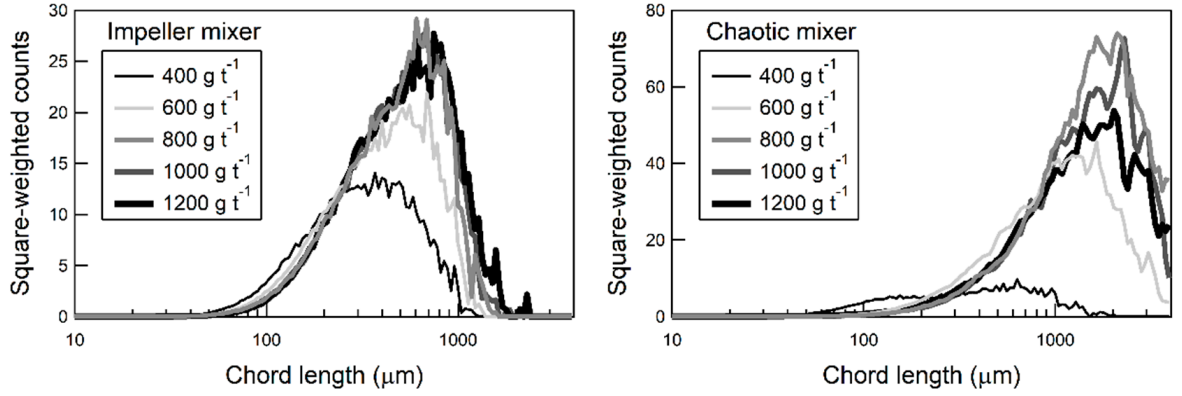

Figure 5. Length square-weighted chord length distributions for 20 wt % kaolin as a function of Magnafloc® 336 dosage for the two mixers.

Figure 6 presents unweighted chord length distributions and the corresponding net water removal measured for an initial kaolin slurry concentration of 30 wt %. The overall trends remain the same,

with the chaotic mixer producing larger aggregate structures and a greater degree of dewatering. However, at the higher initial solids concentration, fines capture in both mixers is suppressed (reflected in higher counts for the 1–10 μm fraction), resulting in lower water recovery. In terms of the larger aggregate structures, the mean square-weighted chord lengths for the impeller and chaotic mixer were 656 μm and 1430 μm, respectively, at a dosage of 1000 g t^{-1}. With both mixers giving poor fines capture, the formation of larger aggregate structures with the chaotic mixer appears to be critical for accelerated dewatering. It should also be noted that the chaotic mixer allowed a decrease in polymer demand (800 g t^{-1}) compared to pitched blade turbine mixing (1000 g t^{-1}) for optimum dewatering.

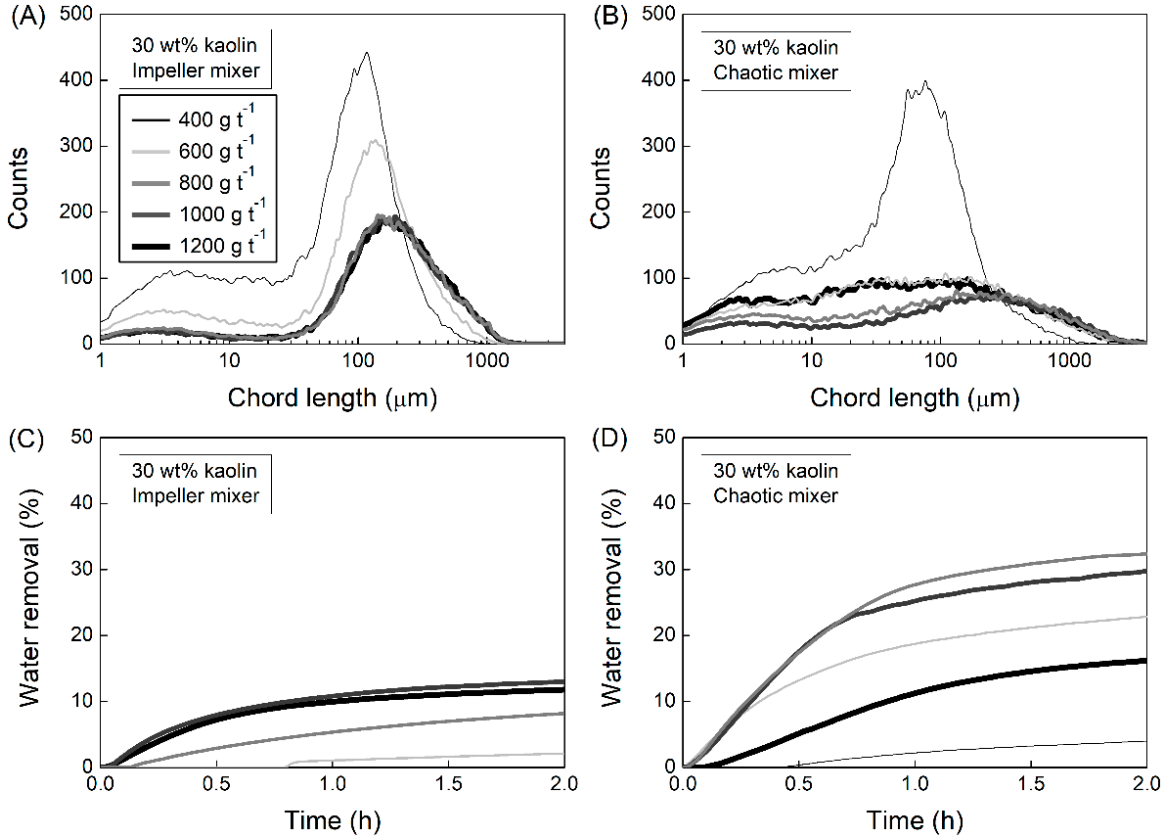

Figure 6. (**A**,**B**) Unweighted chord length distributions for 30 wt % kaolin as a function of Magnafloc® 336 dosage and mixer type. (**C**,**D**) Corresponding net water recovered after 2 h.

For a 35 wt % kaolin suspension (not shown), sediment from the impeller mixer displayed no dewatering over the range of applied dosages, whereas the chaotic mixer gave a maximum water recovery of 22%. These results demonstrate that applying appropriate shear when mixing dense suspensions and viscous polymer solutions is important in optimizing aggregate properties for maximum dewatering. Insufficient or excessive shear leads to structures with reduced permeability and sub-optimal dewatering.

The formation of a highly permeable sediment through aggregate structure alteration allows for the rapid separation of water from the solids. Figure 7 shows the solids concentration measured after dewatering as a function of mixing regime and polymer dosage for two initial kaolin concentrations. It was evident that sediment with a higher dewaterability could be produced using the chaotic mixer compared to the more intense impeller mixing, with the latter giving only marginal additional sediment compaction.

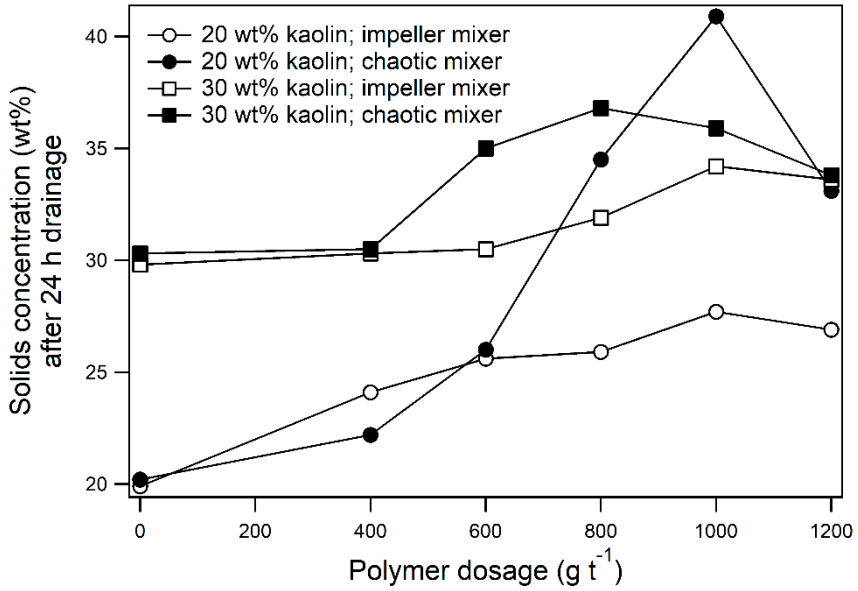

Figure 7. Effect of initial kaolin concentration, Magnafloc® 336 dosage, and mixer type on the solids concentration after 24-h drainage.

3.1.2. Aggregate Free Settling Rates and Effective Densities

The additional water release achieved on deposition after applying high polymer dosages implies the formation of aggregate structures that are denser than those formed from conventional low solids flocculation. The FBRM results regarding the extent of aggregation described in the previous section do not themselves offer any insight on the structure of the aggregates formed. Therefore, samples of the aggregates formed were examined with the FDA. Figure 8A shows the relationship between unhindered free settling velocities and size for approximately 400 individual aggregates produced in the two mixers and collected from the sediment after dewatering measurements. Although there is considerable variation in the data (due to the polydisperse nature of the primary particles and the highly asymmetric aggregates shapes formed), the difference in the fitted curves for aggregates produced by the chaotic and impeller mixer is clearly substantial (approximately 20 m h^{-1} for aggregate sizes of 600 μm). Such a differential in settling velocity has not been observed for low solids flocculation (i.e., as in a thickener feedwell) across a range of conditions and with different flocculant chemistries [30–34].

The size and settling velocity of an aggregate can be used to estimate an effective density, as discussed in Section 2.3.2, although it is recognized that many of the aggregates measured have settling velocities outside the Stokes' regime (approximately 50% of aggregates for the chaotic mixer; 20% for the impeller mixer). While the assumptions made for this calculation may influence the absolute numbers, an inescapable conclusion is that significantly denser aggregate structures are formed under low shear mixing conditions at high polymer dosages.

Figure 8B shows distinct differences in the density–size relationship of the individual aggregates present in the two sediment samples. For example, the average effective density of 200 μm aggregates present in the sediment from the chaotic mixer is 1.28 g cm^{-3}, whereas that from highly turbulent mixing is 1.07 g cm^{-3}. This corresponds (using a particle density of 2.68 g cm^{-3}) to respective volumetric liquor/solid ratios of 5:1 and 23:1. Over the entire range of aggregate sizes measured, higher densities were always recorded for aggregates produced under low shear conditions. This finding suggests that the enhanced dewatering induced by chaotic advection occurred not only by the removal of inter-aggregate water but also by the removal of intra-aggregate water, resulting in densification of the aggregates.

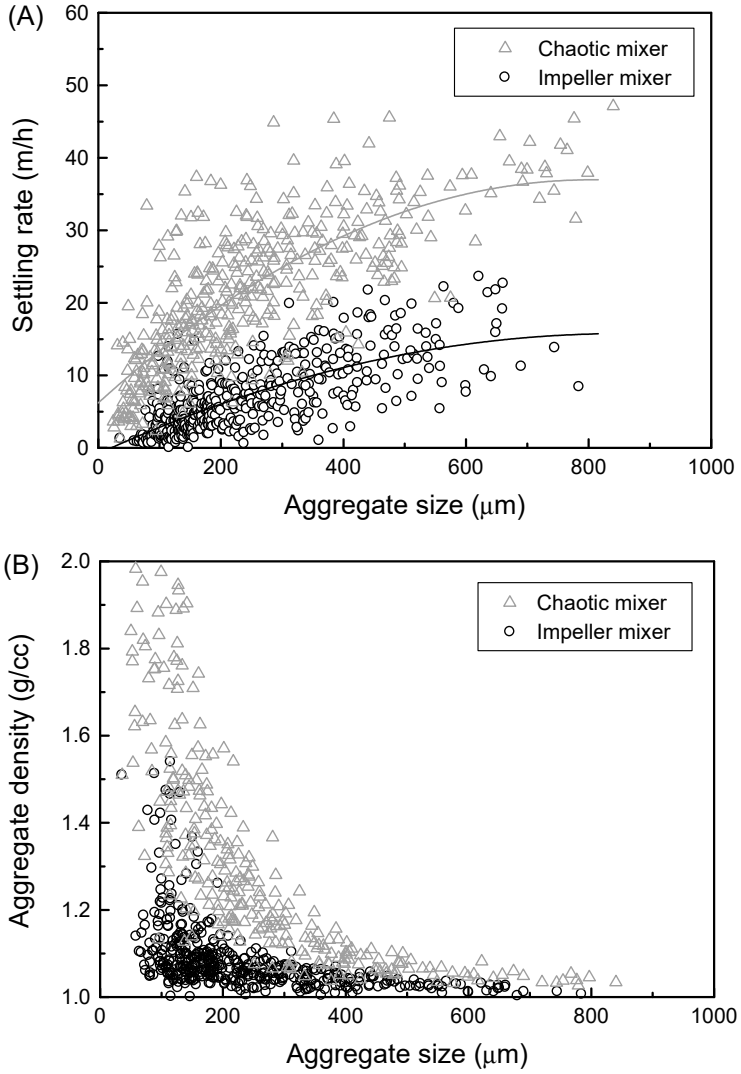

Figure 8. (**A**) Unhindered free settling rates as a function of aggregate size for the two mixer types. Conditions: 30 wt % kaolin, 1000 g t^{-1} Magnafloc® 336. (**B**) Corresponding effective aggregate densities.

Given the impact aggregate structure has on dewatering performance, efforts were made to provide additional characterization. FDA and PVM images both offer insight into the overall morphology of the aggregates. Figures 9 and 10 present comparisons of aggregates produced with the impeller and chaotic mixers, respectively, with images selected to show similarly sized and shaped aggregates for the two techniques. Aggregates formed in the impeller mixer appear less compact and show more filaments or protuberances than those in the chaotic mixer. In contrast to the impeller mixer, aggregate sizes larger than 1 mm were routinely observed during FDA image analysis for the low shear chaotic mixer, which is consistent with results from real-time FBRM monitoring. This supports the assumption that aggregates were not overly damaged or modified by the offline PVM and FDA testing procedures.

These initial measurements suggest that chaotic advection represents a viable approach to polymer dispersion and aggregate growth in tailings underflow applications. This class of mixer shows distinct promise on the grounds upon which mixing is achieved: it is not driven by the dynamics of the flow field itself, but rather through the underlying geometry of the mixing device. Thus, chaotic or topological mixers impart such actions regardless of the material rheology or flowrate, and so mixing is expected to be robust across a wide range of processing conditions.

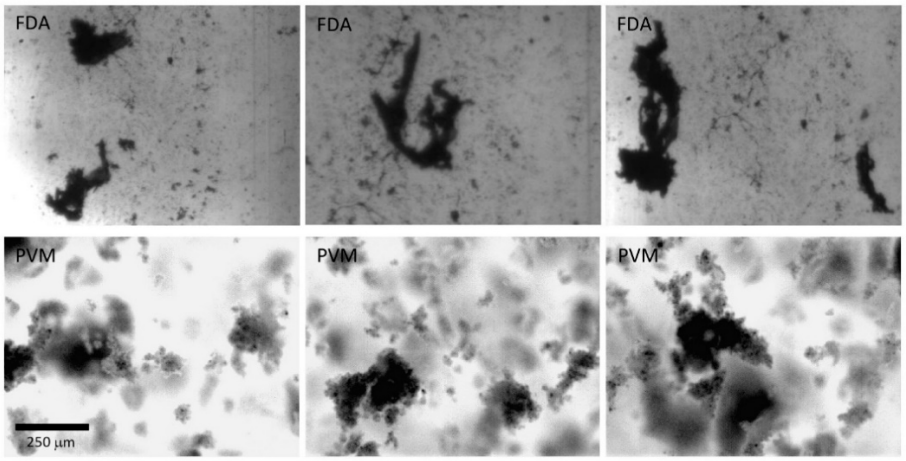

Figure 9. Comparison of FDA and PVM images for aggregates produced in the impeller mixer. Conditions: 30 wt % kaolin, 1000 g t^{-1} Magnafloc® 336. The PVM images were manipulated to enhance contrast and the color was inverted to simulate back-lighting conditions.

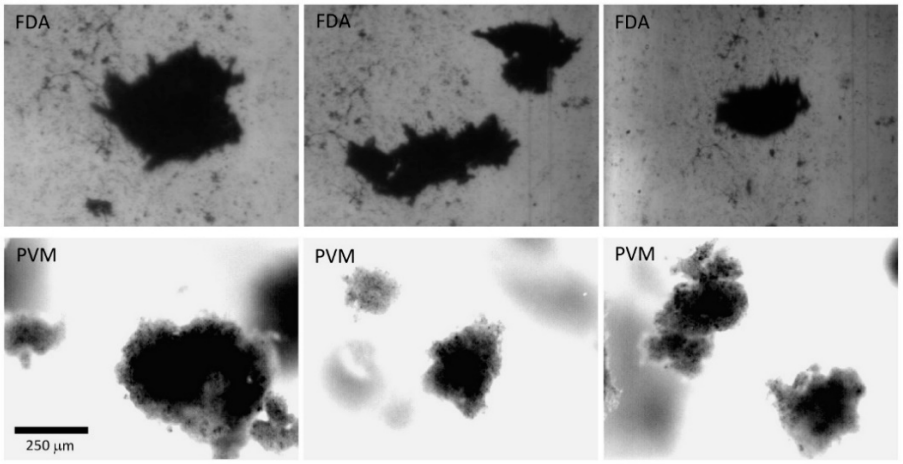

Figure 10. Comparison of FDA and PVM images for aggregates produced in the chaotic mixer. Conditions: 30 wt % kaolin, 1000 g t^{-1} Magnafloc® 336. The PVM images were manipulated to enhance contrast and the color was inverted to simulate back-lighting conditions.

3.2. Tapered Shear and Chaotic Mixing

3.2.1. The Importance of Tapered Shear

In recognition of the difficulty of getting good dispersion of polymer through a high solids suspension, Wells et al. [10] emphasized the importance of adding flocculant under high shear, with subsequent tapered shear to give the optimum discharge properties. The concept is well understood in low solids concentration water treatment applications [35,36], and while not widely recognized as such in the minerals industry, it also forms the basis for the optimal flocculation in well-designed and operated thickener feedwells [34]. A weakness of the chaotic mixing system as applied in Section 3.1 is that polymer is dosed at a single location under mild shear, and hence there is less efficient initial distribution through the suspension at a critical stage when the polymer is most active for adsorption. A pre-conditioning coil was instead introduced to provide a brief period (approximately 10 s) of higher shear (Figure 3), based on the configuration described by Grabsch et al. [37]. Then, the entire system was able to be used in continuous mode, with the chaotic mixer providing consistent low shear across the vessel's full volume to maximize aggregate growth under controlled conditions.

Using tapered shear, distinctly robust aggregate structures were produced that rapidly released water on deposition, with the effects of better fines capture and larger sizes often achieved at lower dosages (Figure 11). The latter was evident through an increase in the mean square-weighted chord lengths from 674 to 2008 µm after the introduction of a short coil ahead of the chaotic mixer, which then minimized any additional shear forces on the existing pre-aggregated material. The water recoveries after 24 h of gravity drainage with and without this tapered shear mixing regime were 74% and 30%, respectively, and the corresponding final solids concentrations were 44.3 and 30.8 wt %.

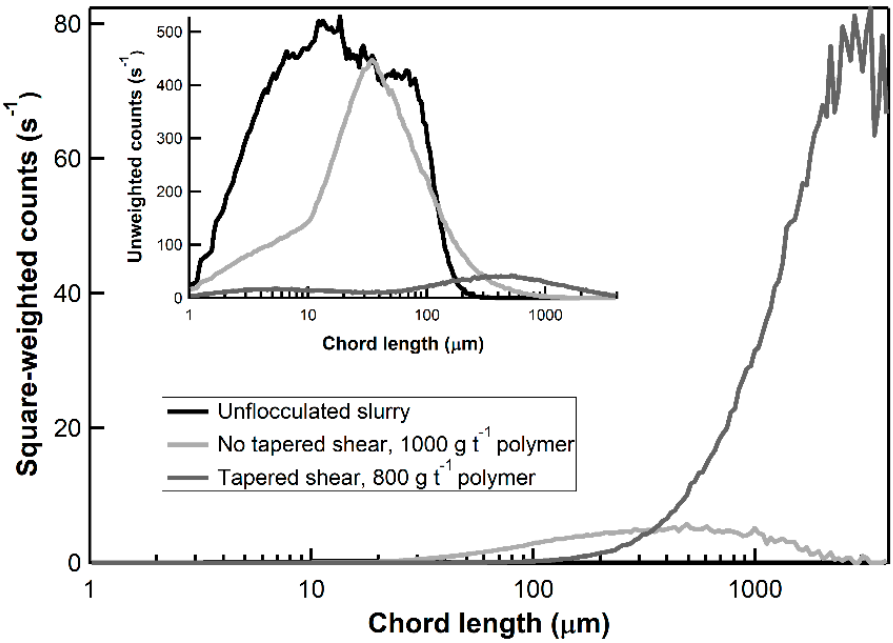

Figure 11. Effect of tapered shear on the unweighted and length square-weighted chord length distributions from focused beam reflectance measurement (FBRM) monitoring of 20 wt % kaolin slurry treated with a high molecular weight (MW) polyacrylamide (PAM) ([η] 17.2 dL g^{-1}).

3.2.2. The Impact of Polymer Molecular Weight

Molecular weight (MW) is a key characteristic governing the effectiveness of water-soluble polymers used in hydrometallurgical or mineral processing operation to induce the aggregation (flocculation) of fine particle suspensions [38,39]. This is primarily a consequence of increased capacity for polymer bridging between particles for higher MW polymers. An increase in MW leads to an increase in coil dimensions that is dependent upon the conformation of the polymer in solution. Larger polymer chains have more potential points of attachment per molecule, while an extended solution conformation increases the probability of successful collisions.

There is very little information in the open literature on the effect of polymer MW on dewatering performance that is of direct relevance to high-solids tailings applications. It is possible that lower MW polymers than those commonly used in thickener feedwells will offer some advantages, although high MW polymers will still be required, as bridging mechanisms are likely to be involved. Of the limited studies available, Watson et al. [40] reported that blends of a very low and a high-MW anionic copolymer could enhance dewatering and consolidation compared with tailings treated by the high-MW polymer alone, producing a trafficable material in less time.

Figure 12A shows the effect of polymer dosage on water recoveries from high-solids kaolin suspensions treated with PAMs of varying MW. For all polymers studied, dosages up to 600 g t^{-1} were ineffective at producing the sought-after continuous networked structure. The highest water returns (approximately 70%) were observed for medium-high MW PAMs ([η] 15–17 dL g^{-1}) at 800 g t^{-1}, with further increases in dosage resulting in diminished returns. Lower MW polymers gave similar

water returns to the higher MW polymers, albeit at elevated dosages (>1000 g t^{-1}), and these were less sensitive to over-dosing. That these experiments used suspensions containing 0.005 M Ca^{2+}, which were shown to have a particularly adverse effect on low MW PAM activity in feedwell flocculation [41,42], highlights the fundamental points of difference between the two processes. Even though low MW chains have fewer potential points of attachment per molecule, the concentrated particle stream in high-solids applications increases the probability of successful collisions under low-shear conditioning.

In Figure 12B, the effect of mixing time on dewaterability is examined at a fixed dosage of 800 g t^{-1}. From this analysis, it is clear the polymers have distinct mixing requirements. The results indicate higher MW polymers that produce more bridges will tolerate and probably require more mixing during inline polymer addition. Fixing the mixing regime on the basis of what is considered appropriate for a low MW polymer may lead to sub-optimal performance for a high MW polymer that is more a reflection of the mixing than the polymer's potential performance.

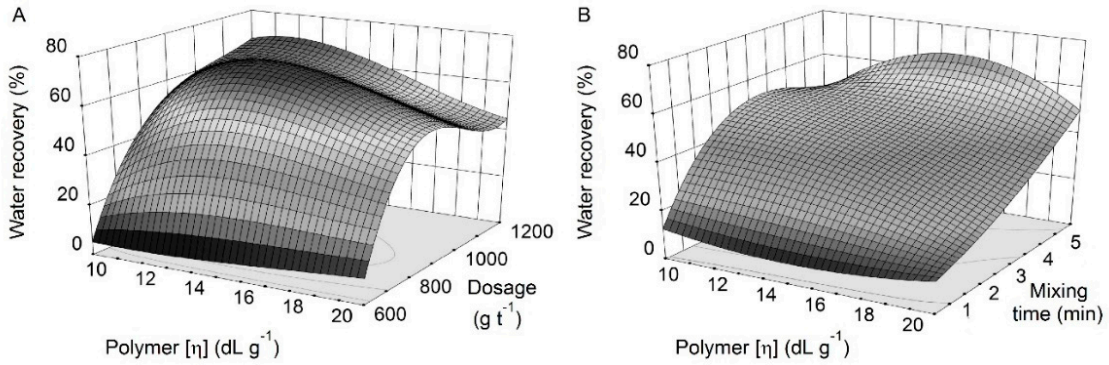

Figure 12. Polyacrylamide (PAM) water recoveries as a function of (**A**) dosage at a mixing time of 5 min, and (**B**) mixing time at a dosage of 800 g t^{-1}. [Ca^{2+}] 0.005 M, 20 wt % kaolin suspensions.

In tailings storage facilities (TSFs), where thickened suspensions are normally held for many years, the compressibility will play a key role in the final achievable solids. Figure 13 shows the compressive yield stress curves for 20 wt % kaolin before and after treatment with low, medium, and very high MW PAMs at 600–1200 g t^{-1}. Increasing the applied dosage resulted in a higher compressive yield stress relative to the untreated suspension (except for the low MW polymer at 600 g t^{-1}). The magnitude of this effect was greatest for the low and medium MW polymers, with the very high MW polymer showing only marginal increases at higher dosages. Above 800 g t^{-1}, the medium MW polymer produced thickened suspension with a significantly higher compressive yield stress than the other polymers, which is consistent with the formation of stronger, more rigid aggregate structures that rapidly expel water. The implication for TSFs is that the compressive yield stress must be exceeded by the self-weight of the over-laying material for the tailings to then consolidate.

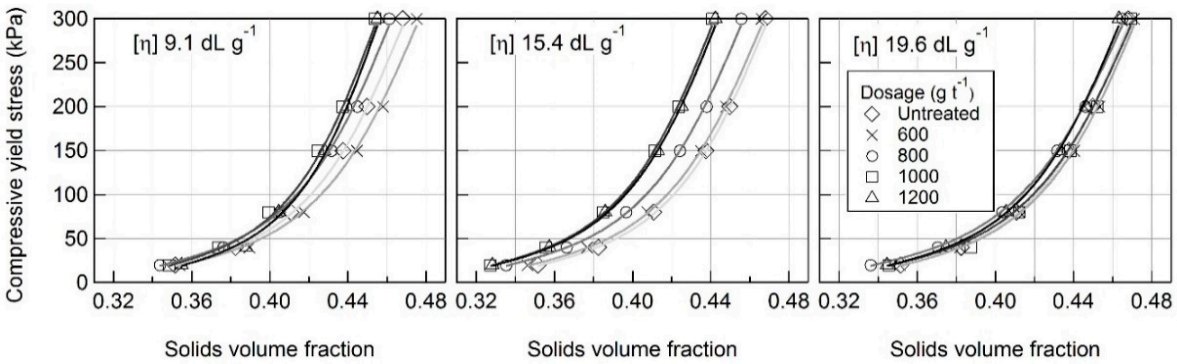

Figure 13. Compressive yield stress curves as a function of PAM [η] and dosage.

3.3. Relating Polymer Performance to Rheological Properties

Medium-to-high MW PAMs ([η] 15–18 dL g^{-1}) were generally preferred for higher water recovery, with diminished performance always observed for the very high MW PAM ([η] 19.6 dL g^{-1}), as shown in Figure 12. This could be caused by entanglements or agglomeration of the polymer chains (non-permanent change) as they flow through transfer pipes, which can impact polymer performance [43].

To test for conformational effects, the viscoelastic properties of the seven PAM solutions (0.1 wt%) were measured using an oscillatory shear rheometer in the frequency range of 0.1 to 100 rad s^{-1}. Figure 14 shows the storage modulus, G′ (elastic response), and loss modulus, G″ (viscous response) of the PAM solutions. For a given frequency, G′ and G″ generally increase with MW for the series of polymers studied, although the highest MW PAM ([η] 19.6 dL g^{-1}), which was presented as a dashed gray line, is an exception to this, presumably because its polymer chains are highly entangled. Crucially, the results illustrate that the direct measurement of viscoelastic properties provides a better indication of a polymer's potential performance than intrinsic viscosity [η].

It is noteworthy that the magnitude of the difference between PAM 12.2 and PAM 15.4 in Figure 14 was less pronounced for measurements carried out with 0.5 wt % polymer solutions (not shown). This concentration-dependence in the dynamic moduli suggests that a critical polymer concentration (C*) exists beyond which the rate of change in G′ and G″ rapidly increases. At higher concentrations, more chains are available, thus increasing the probability of association/interaction between polymer chains. Decreasing polymer MW would lead to an increase in C* as it directly impacts the polymer's chain size and radius of gyration.

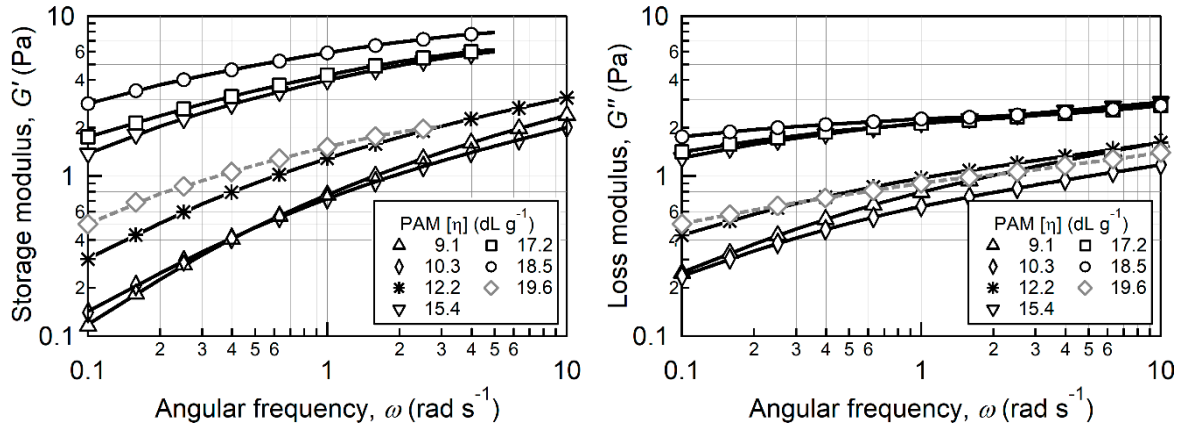

Figure 14. Linear viscoelastic properties of the anionic PAM solutions (adapted from [41]; copyright (2018) with permission from Elsevier).

Oscillatory tests would be expected to provide more information than intrinsic viscosity tests because the tests probe both the amount of energy stored by the deformable polymers (via G′) and the dissipative behavior of the polymers in solution (via G″). Both these measures are able to be made across a range of frequencies, in contrast to [η], which gives a measure of the hydrodynamic size in the limit of zero concentration and zero shear. Bridging and related flocculation mechanisms depend on the molecular size, concentration, conformation, and deformability. Therefore, the enhanced information provided by oscillatory measurements compared with [η] should provide greater insights into polymer performance prediction.

4. Implications

A challenge in studies of high molecular weight polymers used for the aggregation of fine particle suspensions is to design experiments in such a way as to properly isolate polymer impacts from that of the applied shear regime used to induce aggregation. This may not be a major concern in wastewater

clarification studies at very low solids concentrations, for which quite strong mixing in traditional jar tests (i.e., impeller mixed vessels) is required to promote aggregating collisions between particles, with reaction times measured in minutes. Aggregation is more sensitive to applied shear conditions at moderate and high solids concentrations, with required reaction times far shorter and, critically, the likelihood that extended durations under shear will be highly detrimental [44].

Excessive shear in such tests can dampen or mask performance trends, as may be the case in results from Clark et al. [45], who attempted to quantify the effects of both flocculant molecular weight and anionic charge density on settling rates for kaolin at moderate solids concentrations, but consistently applied a protocol of 20 cylinder inversions identified previously with lower molecular weight cationic flocculants [46]. This was likely to be excessive shear for anionic flocculants and certainly for higher molecular weight products. The published literature related to polymer dosing at higher solids concentrations suffers such issues to a greater degree, with the authors in many cases even admitting to testing polymers at below the target solids concentrations because of their inability to get useful results without solids dilution. The consequences can be extreme overdosing [47], ill-defined mixing conditions [48], or the contrasting of distinct products under inappropriate shear and dosing regimes [12].

The system described here involving continuous flow through a pre-conditioning coil followed by a chaotic mixer offers excellent control over both the high shear applied during the initial mixing of the polymer solution and the subsequent lower shear used to achieve a maximum aggregate size prior to deposition. Such control has never been achieved in any previous published study of polymer dosing at high solids concentrations, and this preparative approach has clear advantages in terms of offering insights into both the impacts of polymer properties and the optimization of applied conditions. However, the disadvantage of this is in the requirement for attaining much larger suspension volumes, with the treatment of at least 6 L (approximately 3 turnovers of the entire system volume) at each condition essential to ensure stability. While this may seem excessive in cases where the preparation of only small volumes is sought for micro-characterization, scaling down the dimensions of the equipment is not recommended. Then, flow within the pre-conditioning coil may become unstable, and reducing the gaps between the rods within the chaotic mixer could potentially impact upon the size of aggregates that can be formed.

Mixing into high solids streams at an industrial scale is also disadvantaged by the energy costs associated with the highly viscous nature of the thickener underflows and large processing volumes. To address this, new mixing techniques need to be developed that can be applied to rheologically complex materials, impart low shear, and consume low energy, for which chaotic advection is an option. The chaotic mixer described here clearly could not be scaled up appropriately to be applied industrially, particularly given the complexity of the rod rotation, which would represent a high capital cost. However, Lester and Chryss [49] have described a static mixing device inspired by bakers' flow [50], which is a three-dimensional fluid mechanical analog of the bakers' map that is used for the study of chaos in dynamical systems. This device has been shown to give rapid, efficient global mixing over a range of yield stress fluids ranging from viscous- to plastic-dominated.

In separate work, the chaotic mixer was used to dewater a challenging industrial clay slurry containing palygorskite, which is a magnesium aluminium phyllosilicate that is present in many calcrete-hosted uranium and rare-earth metal deposits. The stability of this slurry is attributed to the distribution of alternating positive and negative charges on the extremely acicular palygorskite particles, which readily form gel suspensions in salt and fresh water. Pre-aggregation in the conditioning coil strongly affected the subsequent breakdown of the gel structure by the gentle stretching and folding motion imparted by the rotating rods. Crucially, experiments carried out under the same conditions with an axial flow impeller mixer failed to produce a well-flocculated structure for a wide range of flocculant types and dosages. The results from this case study will be reported elsewhere.

5. Conclusions

This work has demonstrated that the addition of polymer solutions to high solids kaolin suspensions under the low shear conditions imparted by chaotic advection resulted in markedly improved dewatering performance and enhanced consolidation. The application of a suite of aggregate measurement tools (FBRM, FDA, and PVM) revealed the formation of a larger, denser aggregate structure compared to a common bench-top mixing practice. These reflected in at least a doubling of the mean square-weighted chords lengths (approximately 1500 μm versus 600 μm), significantly higher free settling rates of individual aggregates (20 m h^{-1} versus 6 m h^{-1} for 200 μm aggregates), and higher corresponding effective densities (1.28 g cm^{-3} versus 1.07 g cm^{-3}). The controlled formation of optimal aggregate structures by chaotic advection could result in improved water recovery by reducing the water lost in tailings through evaporation and entrapment.

Access to seven anionic PAMs with distinct MWs, coupled with specialized tools for flocculation under controlled conditions and real-time measurement of aggregate dimensions, has produced new insights into how process variables substantially alter the flocculation response to MW. Across the high-solids regime, medium-to-high MW polymers were generally preferred, with further increases in MW resulting in significantly diminished dewatering outcomes. Importantly, direct analysis of these specific polymer solutions through oscillatory rheology provides a more robust basis for flocculant selection, which is currently very much trial and error.

Further work is required to develop in-line methods for underflow polymer mixing in tailings management applications across the broad range of relevant processing conditions.

Author Contributions: Conceptualization, A.C. (Andrew Chryss); methodology, A.C. (Allan Costine) and A.C. (Andrew Chryss); validation, A.C. (Allan Costine) and A.C. (Andrew Chryss); formal analysis, A.C. (Allan Costine) and A.C. (Andrew Chryss); investigation, A.C. (Allan Costine) and A.C. (Andrew Chryss); resources, S.D. and J.B.; data curation, A.C. (Allan Costine) and A.C. (Andrew Chryss); writing—original draft preparation, A.C. (Allan Costine); writing—review and editing, P.F., A.C. (Andrew Chryss) and J.B.; visualization, A.C. (Allan Costine) and S.D.; supervision, A.C. (Andrew Chryss) and P.F.; project administration, A.C. (Andrew Chryss) and P.F.; funding acquisition, A.C. (Andrew Chryss) and P.F. All authors have read and agreed to the published version of the manuscript.

Funding: The financial support of Anglo Operations, BASF, Freeport McMoran, Gold Fields, Nalco, Newmont, Outotec, Shell Canada Energy, and Total E&P Canada through the AMIRA P1087 Integrated Tailings Management is gratefully acknowledged, along with support from CSIRO Mineral Resources.

Acknowledgments: We thank Neil Francis and Greta Brodie (CSIRO) for help with the FDA software and PVM analysis, respectively, and Dan Lester (RMIT University) for useful discussions on the chaotic advection approach. Alex Lubansky, James Cox, and Shaun Travaglini (all formerly of Edith Cowan University) are thanked for carrying out the oscillatory rheology experiments.

Conflicts of Interest: The authors declare no conflict of interest.

References

1. Davies, M.P.; Lupo, J.; Martin, T.; McRoberts, E.; Musse, M.; Ritchie, D. Dewatered tailings practice—Trends and observations. In Proceedings of the Fourteenth International Conference on Tailings and Mine Waste, Vail, Colorado, 17–20 October 2010; Taylor & Francis: London, UK; pp. 133–142.
2. Fourie, A.B. Perceived and realised benefits of P&TT for surface deposition. In Proceedings of the 15th International Seminar on Paste and Thickened Tailings (Paste 2012), Sun City, South Africa, 16–19 April 2012; Jewell, R.J., Fourie, A.B., Paterson, A., Eds.; Australian Centre for Geomechanics: Nedlands, Australia; pp. 53–64.
3. Williams, M.P.A.; Seddon, K.D.; Fitton, T.G. Surface disposal of paste and thickened tailings—A brief history and current confronting issues. In Proceedings of the 11th International Seminar on Paste and Thickened Tailings (Paste 2008), Kasane, Botswana, 5–9 May 2008; Fourie, A., Jewell, R., Slatter, P., Paterson, A., Eds.; Australian Centre for Geomechanics: Nedlands, Australia; pp. 143–164.
4. Bedell, D.; Slottee, S.; Shoenbrunn, F.; Fawell, P. Chapter 7—Thickening. In *Paste and Thickened Tailings—A Guide*, 3rd ed.; Jewell, R.J., Fourie, A.B., Eds.; Australian Centre for Geomechanics: Nedlands, Australia, 2015; pp. 113–136.

5. Cooling, D.J. Improving the sustainability of residue management practices—Alcoa World Alumina Australia. In Proceedings of the 10th International Seminar on Paste and Thickened Tailings (Paste 2007), Perth, Australia, 13–15 March 2007; Fourie, A., Jewell, R.J., Eds.; Australian Centre for Geomechanics: Nedlands, Australia; pp. 3–16.
6. Hogg, R. Flocculation and dewatering. *Int. J. Min. Process.* **2000**, *58*, 223–236. [CrossRef]
7. Kaminsky, H.A.W.; Etsell, T.H.; Ivey, D.G.; Omotoso, O. Distribution of clay minerals in the process streams produced by the extraction of bitumen from athabasca oil sands. *Can. J. Chem. Eng.* **2009**, *87*, 85–93. [CrossRef]
8. McColl, P.; Scammell, S.; Philip, M.; Stephen, S. Treatment of Mineral Material, Especially Waste Mineral Slurries Transferring Material with Dispersed Particulate Solids as Fluid to Deposition Area by Combining with Material Aqueous Solution of Water-Soluble Polymer. Numerous Country Patents WO2004060819-A1 WOEP000042, 7 January 2004.
9. Gaillard, N.; Poncet, F. Treating Sludge from Mining or Mineral Industry before Spreading out into Soil, Comprises Contacting the Sludge with a Branched Flocculant such as a Water Soluble Organic Polymer Having a Specified Anionicity for a Specified Duration. Patent FR2937635-A1; US2010105976-A1; CA2682542-A1, 29 April 2010.
10. Wells, P.S.; Revington, A.; Omotoso, O. Mature fine tailings drying—Technology update. In Proceedings of the 14th International Seminar on Paste and Thickened Tailings (Paste 2011), Perth, Australia, 5–7 April 2011; Jewell, R., Fourie, A., Eds.; Australian Centre for Geomechanics: Nedlands, Australia; pp. 155–166.
11. Fawell, P. Solid-liquid separation of clay tailings. In *Clays in the Minerals Processing Value Chain*; Gräfe, M., Klauber, C., McFarlane, A.J., Robinson, D., Eds.; Cambridge University Press: Cambridge, UK, 2017; pp. 327–380.
12. Botha, L.; Davey, S.; Nguyen, B.; Swarnakar, A.K.; Rivard, E.; Soares, J.B.P. Flocculation of oil sands tailings by hyperbranched functionalized polyethylenes (HBfPE). *Min. Eng.* **2017**, *108*, 71–82. [CrossRef]
13. Vajihinejad, V.; Soares, J.B.P. Monitoring polymer flocculation in oil sands tailings: A population balance model approach. *Chem. Eng. J.* **2018**, *346*, 447–457. [CrossRef]
14. Vedoy, D.R.L.; Soares, J.B.P. Water-soluble polymers for oil sands tailing treatment: A Review. *Can. J. Chem. Eng.* **2015**, *93*, 888–904. [CrossRef]
15. Zhang, D.; Thundat, T.; Narain, R. Flocculation and dewatering of mature fine tailings using temperature-responsive cationic polymers. *Langmuir* **2017**, *33*, 5900–5909. [CrossRef] [PubMed]
16. Lester, D.R.; Rudman, M.; Metcalfe, G. Low Reynolds number scalar transport enhancement in viscous and non-Newtonian fluids. *Int. J. Heat Mass Transf.* **2009**, *52*, 655–664. [CrossRef]
17. Metcalfe, G.; Rudman, M. Fluid Mixer. International Patent WO 02/20144A1, 13 June 2002.
18. Metcalfe, G.; Rudman, M.; Brydon, A.; Graham, L.J.W.; Hamilton, R. Composing chaos: An experimental and numerical study of an open duct mixing flow. *Alche J.* **2006**, *52*, 9–28. [CrossRef]
19. Speetjens, M.; Metcalfe, G.; Rudman, M. Topological mixing study of non-Newtonian duct flows. *Phys. Fluids* **2006**, *18*, 103103. [CrossRef]
20. Finn, M.D.; Thiffeault, J.L. Topological entropy of braids on the torus. *Siam J. Appl. Dyn. Syst.* **2007**, *6*, 79–98. [CrossRef]
21. Finn, M.D.; Thiffeault, J.L. Topological optimization of rod-stirring devices. *Siam Rev.* **2011**, *53*, 723–743. [CrossRef]
22. Bagusat, F.; Böhme, B.; Schiller, P.; Mögel, H.J. Shear induced periodic structure changes in concentrated alumina suspensions at constant shear rate monitored by FBRM. *Rheol. Acta* **2005**, *44*, 313–318. [CrossRef]
23. Richmond, W.R.; Jones, R.L.; Fawell, P.D. The relationship between particle aggregation and rheology in mixed silica-titania suspensions. *Chem. Eng. J.* **1998**, *71*, 67–75. [CrossRef]
24. Heath, A.R.; Fawell, P.D.; Bahri, P.A.; Swift, J.D. Estimating average particle size by focused beam reflectance measurement (FBRM). *Part. Part. Syst. Char.* **2002**, *19*, 84–95. [CrossRef]
25. Senaputra, A.; Jones, F.; Fawell, P.D.; Smith, P.G. Focused beam reflectance measurement for monitoring the extent and efficiency of flocculation in mineral systems. *Alche J.* **2014**, *60*, 251–265. [CrossRef]
26. The Next Generation FBRM® (Focused Beam Reflectance Measurement). Mettler-Toledo Autochem. Available online: https://www.mt.com (accessed on 23 June 2020).

27. Farrow, J.B.; Warren, L.J. *Measurement of the Size of Aggregates in Suspension*; Coagulation and Flocculation—Theory and Application; Dobias, B., Ed.; Marcel Dekker: New York, NY, USA, 1993; pp. 391–426.
28. Happel, J.; Brenner, H. *Low Reynolds Number Hydrodynamics*; Noordhoff International Publishing: Leyden, The Netherlands, 1973.
29. Usher, S.P.; De Kretser, R.G.; Scales, P.J. Validation of a new filtration technique for dewaterability characterization. *Alche J.* **2001**, *47*, 1561–1570. [CrossRef]
30. Benn, F.A.; Fawell, P.D.; Halewood, J.; Austin, P.J.; Costine, A.D.; Jones, W.G.; Francis, N.S.; Druett, D.C.; Lester, D. Sedimentation and consolidation of different density aggregates formed by polymer-bridging flocculation. *Chem. Eng. Sci.* **2018**, *184*, 111–125. [CrossRef]
31. Costine, A.D.; Vajihinejad, V.; Botha, L.; Fawell, P.D.; Soares, J.B.P. Aggregate structures formed by hyperbranched functionalized polyethylene (HBfPE) treatment of oil sands tailings. *Can. J. Chem. Eng.* **2019**, *97*, 99–102. [CrossRef]
32. Farrow, J.B.; Johnston, R.R.M.; Simic, K.; Swift, J.D. Consolidation and aggregate densification during gravity thickening. *Chem. Eng. J.* **2000**, *80*, 141–148. [CrossRef]
33. Kyoda, Y.; Costine, A.D.; Fawell, P.D.; Bellwood, J.; Das, G.K. Using focused beam reflectance measurement (FBRM) to monitor aggregate structures formed in flocculated clay suspensions. *Min. Eng.* **2019**, *138*, 148–160. [CrossRef]
34. Owen, A.T.; Fawell, P.D.; Swift, J.D.; Labbett, D.M.; Benn, F.A.; Farrow, J.B. Using turbulent pipe flow to study the factors affecting polymer-bridging flocculation of mineral systems. *Int. J. Min. Process.* **2008**, *87*, 90–99. [CrossRef]
35. Nan, J.; He, W. Characteristic analysis on morphological evolution of suspended particles in water during dynamic flocculation process. *Desalin. Water Treat.* **2012**, *41*, 35–44. [CrossRef]
36. Yukselen, M.A.; O'Halloran, K.R.; Gregory, J. Effect of tapering on the break-up and reformation of flocs formed using hydrolyzing coagulants. *Water Sci. Technol. Water Supply* **2006**, *6*, 139–145. [CrossRef]
37. Grabsch, A.F.; Fawell, P.D.; Adkins, S.J.; Beveridge, A. The impact of achieving a higher aggregate density on polymer-bridging flocculation. *Int. J. Min. Process.* **2013**, *124*, 83–94. [CrossRef]
38. Li, H.; Long, J.; Xu, Z.; Masliyah, J.H. Effect of molecular weight and charge density on the performance of polyacrylamide in low-grade oil sand ore processing. *Can. J. Chem. Eng.* **2008**, *86*, 177–185. [CrossRef]
39. Proskurina, V.E.; Myagchenkov, V.A. Flocculation activity of anionic copolymers of acrylamide with respect to titanium dioxide suspension as influenced by their molecular properties. *Russ. J. Appl. Chem.* **2006**, *79*, 301–305. [CrossRef]
40. Watson, P.; Farinato, R.; Fenderson, T.; Hurd, M.; Macy, P.; Mahmoudkhani, A. Novel polymeric additives to improve oil sands tailings consolidation. In Proceedings of the SPE International Symposium on Oilfield Chemistry, The Woodlands, TX, USA, 11–13 April 2011; pp. 703–709.
41. Costine, A.; Cox, J.; Travaglini, S.; Lubansky, A.; Fawell, P.; Misslitz, H. Variations in the molecular weight response of anionic polyacrylamides under different flocculation conditions. *Chem. Eng. Sci.* **2018**, *176*, 127–138. [CrossRef]
42. Witham, M.I.; Grabsch, A.F.; Owen, A.T.; Fawell, P.D. The effect of cations on the activity of anionic polyacrylamide flocculant solutions. *Int. J. Min. Process.* **2012**, *114–117*, 51–62. [CrossRef]
43. Owen, A.T.; Nguyen, T.V.; Fawell, P.D. The effect of flocculant solution transport and addition conditions on feedwell performance in gravity thickeners. *Int. J. Min. Process.* **2009**, *93*, 115–127. [CrossRef]
44. Jeldres, R.I.; Fawell, P.D.; Florio, B.J. Population balance modelling to describe the particle aggregation process: A review. *Powder Technol.* **2018**, *326*, 190–207. [CrossRef]
45. Clark, A.Q.; Herrington, T.M.; Petzold, J.C. The flocculation of kaolin suspensions with anionic polyacrylamides of varying molar mass and anionic character. *Colloids Surf.* **1990**, *44*, 247–261. [CrossRef]
46. Gill, R.I.S.; Herrington, T.M. The flocculation of kaolin suspensions with cationic polyacrylamides of varying molar mass but the same cationic character. *Colloids Surf.* **1987**, *22*, 51–76. [CrossRef]
47. Strandman, S.; Vachon, R.; Dini, M.; Giasson, S.; Zhu, X.X. Polyacrylamides revisited: Flocculation of kaolin suspensions and mature fine tailings. *Can. J. Chem. Eng.* **2018**, *96*, 20–26. [CrossRef]
48. Wang, H.; Chao, L.; Wei, X.; Qi, X.; Li, J.; Jiang, L.; Li, W.; Jia, P. Design and preparation of flocculant with self-degrading characteristics for dewatering of oil sand tailings. *J. Disper. Sci. Technol.* **2019**. [CrossRef]

49. Lester, D.R.; Chryss, A. Topological mixing of yield stress materials. *Phys. Rev. Fluids* **2019**, *4*, 064502. [CrossRef]
50. Carrière, P. On a three-dimensional implementation of the baker's transformation. *Phys. Fluids* **2007**, *19*, 118110. [CrossRef]